JACC: CARDIOVASCULAR IMAGING VOL. 2, NO. 9, 2009

ISSN 1936-878X/09/$36.00
PUBLISHED BY ELSEVIER INC. DOI:10.1016/j.jcmg.2009.03.021

ORIGINAL RESEARCH

Evaluation of Left Atrial Degeneration for the Prediction of Atrial Fibrillation

Usefulness of Integrated Backscatter Transesophageal Echocardiography

Tomoki Kubota, MD, Masanori Kawasaki, MD, PhD, Nobuhiro Takasugi, MD, Urara Takeyama, MD, PhD, Yoshiyuki Ishihara, MD, Munenori Okubo, MD, PhD, Takahiko Yamaki, MD, Shinsuke Ojio, MD, PhD, Takuma Aoyama, MD, PhD, Masazumi Arai, MD, PhD, Kazuhiko Nishigaki, MD, PhD, Genzou Takemura, MD, PhD, Hisayoshi Fujiwara, MD, PhD, Shinya Minatoguchi, MD, PhD

Gifu, Japan

OBJECTIVES The purpose of this study was to elucidate the usefulness of integrated backscatter (IBS) transesophageal echocardiography (TEE) for the evaluation of atrial degeneration and clarify whether atrial degeneration predicts the occurrence of atrial fibrillation (AF).

BACKGROUND One of the causes of AF is pathological degeneration of the left atrium (LA). However, there is no appropriate method to evaluate degeneration of the LA in the clinical setting.

METHODS The IBS images were acquired with TEE with a 4- to 7-MHz transducer. The IBS values were calculated as the average power of the backscattered signal from regions of interest (ROI). In the pathological study, we measured IBS values of 21 left atrial specimens obtained from 10 autopsied hearts. Relative interstitial area in the ROI was automatically calculated by a personal computer. In the clinical study, we measured IBS values of the entire LA wall at 5-mm intervals (except the posterior wall) in 42 patients (18 non-AF patients, 14 paroxysmal AF patients, and 10 chronic AF patients). Each IBS value was color-coded to construct 3-dimensional maps.

RESULTS There was a weak correlation between the relative interstitial area and IBS values ($r = 0.45$, $p = 0.038$). Average corrected IBS values of total voxels in color-coded maps in the AF group (24.4 ± 6.4 dB) and the paroxysmal AF group (23.9 ± 9.6 dB) were significantly greater than those in the non-AF group (15.6 ± 7.4 dB, $p = 0.007$), whereas there was no significant difference in LA diameter between the paroxysmal AF group (39.4 ± 6.5 mm) and the non-AF group (36.7 ± 5.5 mm).

CONCLUSIONS With IBS-TEE, we can identify an increase in atrial degeneration that might predict the occurrence of AF before LA dilation. (J Am Coll Cardiol Img 2009;2:1039–47) © 2009 by the American College of Cardiology Foundation

From Regeneration and Advanced Medical Science, Gifu University Graduate School of Medicine, Gifu, Japan.
Manuscript received November 6, 2008; revised manuscript received February 24, 2009, accepted March 9, 2009.

JACC: CARDIOVASCULAR IMAGING, VOL. 2, NO. 9, 2009
SEPTEMBER 2009:1039–47

Atrial fibrillation (AF) is 1 of the most common arrhythmias in the clinical setting. AF is strongly correlated with increasing age and occurs with a prevalence of 5.9% in individuals older than 65 years (1). Although AF is likely to affect quality of life and the hemodynamic status of patients with recognizable heart failure, little is known about the pathological changes in atria that occur before the onset of AF. An autopsy study reported increased amounts of fibrosis in the atria of patients with AF compared with those in sinus rhythm (2). Another study reported that some of the histological features of the left atrium (LA) in patients with AF were an increase in interstitial tissue with infiltration of fatty tissue, interstitial fibrosis, and disruption of atrial muscle (3).

To predict the occurrence of AF it is important to evaluate the degeneration of LA tissue. Investigation of LA tissue characteristics on the basis of atrial biopsies demonstrated abnormal histological features in multiple biopsy specimens in all patients with lone AF (4). However, atrial biopsy requires considerable skill and often results in complications. Therefore, there is no appropriate method to evaluate degeneration of the LA routinely in the clinical setting.

ABBREVIATIONS AND ACRONYMS

AF = atrial fibrillation
ANP = atrial natriuretic peptide
BNP = brain natriuretic peptide
cIBS = corrected integrated backscatter
IBS = integrated backscatter
LA = left atrium
LAA = left atrial appendage
PAF = paroxysmal atrial fibrillation
ROI = region-of-interest
TEE = transesophageal echocardiography

A promising technique to evaluate tissue characteristics in vivo is integrated backscatter (IBS) ultrasound. Previous studies have shown that IBS values obtained from the analysis of ultrasound images of the carotid arteries reflected the acoustic characteristics of the wall and can differentiate the tissue characteristics of arterial plaques (5,6). In the myocardium, IBS values were related with myocardial fibrosis in the patients with cardiomyopathy (7,8). Therefore, we hypothesized that it should be possible to evaluate the degeneration of LA tissue by applying IBS analysis to images from transesophageal echocardiography (TEE).

The purpose of this study was to elucidate the usefulness of IBS-TEE for the evaluation of atrial degeneration and clarify whether atrial degeneration evaluated by IBS-TEE reflects AF.

METHODS

Subjects and study protocol. Forty-two patients (18 non-AF patients, 14 paroxysmal atrial fibrillation patients [PAF], and 10 chronic AF patients) were enrolled in the present study. All patients underwent TEE to evaluate valvular disease or the presence of thrombus in the cardiac chambers. Exclusion criteria include unstable angina or myocardial infarction within the previous 4 weeks, an ejection fraction <30%, chronic heart failure (New York Heart Association functional class >III), mitral valve stenosis (mitral valve area <2 cm^2) or prevalent esophageal varices. Atrial natriuretic peptide (ANP) and brain natriuretic peptide (BNP) were measured, and conventional transthoracic echocardiography was performed at the same time as TEE. Risk factors for coronary artery disease were evaluated in each patient, including diabetes mellitus (medication dependent, including oral hypoglycemic drugs and insulin), hypertension (medication-dependent only), smoking status (current smoker or quit <6 months before the study), and dyslipidemia (medication-dependent only). A Holter electrocardiogram (ECG) was obtained within 2 weeks after TEE in all patients. The study was approved by the ethics committee of Gifu University Hospital, and informed consent was obtained from all patients before enrollment.

Echocardiography and IBS measurement in the clinical study. In the clinical study, left atrial dimension (LAD), left ventricular (LV) end-diastolic dimension, LV ejection fraction, and left atrial appendage (LAA) peak velocity were measured by conventional transthoracic echocardiography. The LA volume was calculated with a method that was recommended for chamber quantification (9). After those measurements, TEE was performed with a 4- to 7-MHz multiplane transducer with a 7.4-mm diameter pediatric probe (SONOS 7500, Philips Medical Systems, Andover, Massachusetts) in the echocardiography laboratory. The oropharynx was anesthetized with lidocaine before TEE. After the cardiac examination, images of the LA were depicted, and IBS values of entire lateral, septal, and anterior walls of the LA were measured at 5-mm intervals with a small region of interest (ROI) (6 × 6 pixels, 0.3 × 0.3 mm) set at each location (Fig. 1). We set the time gain compensation at 70 dB and the lateral gain compensation at 70 dB at every measurement in both the ex vivo and in vivo studies. At this setting, the IBS value of a stainless steel needle at a distance of 4 cm from the transducer was 63 dB. When the frequency of the transducer was 4 to 7 MHz, the resolution was approximately 0.2 to 0.4 mm assuming a sound velocity in tissue of 1,540 m/s. The posterior wall was excluded from the analysis, because the wall was affected by the diffraction and reverberation phenomena due to the

short distance from the probe. In addition, ultrasonic backscatter is angle-dependent, and this might potentially be a limitation to quantitative ultrasonic diagnosis (10). In the IBS measurements of the posterior atrial walls, subcutaneous tissues existing between a transducer and the atrial wall might cause erratic diffraction in addition to the influence of the aforementioned angle dependency in the posterior atrial wall. Therefore, the posterior atrial wall (an angle span of 180° between −90° and +90°) was excluded from the analysis in this study, and the IBS evaluation was performed with just the lateral, septal, and anterior walls. The IBS values of the LA wall were corrected (corrected integrated backscatter [cIBS]) by subtracting the IBS values in the LA cavity near the LA wall. Each IBS value was color coded to construct 3-dimensional (3D) IBS maps of the entire lateral, septal, and anterior walls of the LA. Three-dimensional image construction of LA tissue degeneration was performed by computer software (T3D, Fortner Research LLC, Sterling, Virginia). We employed mean cIBS values of the entire LA wall (except the posterior wall) to evaluate LA degeneration.

Pathological study. Twenty-one left atrial specimens, which were fixed with neutral 10% buffered formalin, obtained from 10 autopsied hearts were used in the pathological study (5). In the ex vivo measurements, the atrial specimen was placed 4 cm from the same transducer as used in the clinical study in a 0.9% saline solution at a temperature of 37°C. The IBS and conventional 2-dimensional echocardiography images were obtained in the same setting used in the clinical study. To clarify the cross-sectional position of the included segment, multiple surgical needles were carefully inserted into the atrial wall to be used as a reference to compare the IBS values with histology. Cross-sectional images from sites containing surgical needles were obtained to ensure that the IBS measurement and histology were compared at the same site. After the images were acquired, imaging sites were sutured by stitches that were attached to the surgical needles to serve as a reference to compare IBS values with histology. This method was successfully used previously to compare histology and ultrasound images of atherosclerotic plaques (5,11). The IBS values of the atrial wall were corrected (cIBS) by subtracting the IBS values of saline just above the LA tissue. Tissue was stained with hematoxylin and eosin and Masson's trichrome. Histological images that were stained with Masson's trichrome were digitized, and the interstitial areas that were not stained blue were automatically selected by a multipurpose image processor (LUZEX F, Nireco Co., Tokyo, Japan). The relative interstitial area (interstitial area/area of ROI) was automatically calculated by the LUZEX F system.

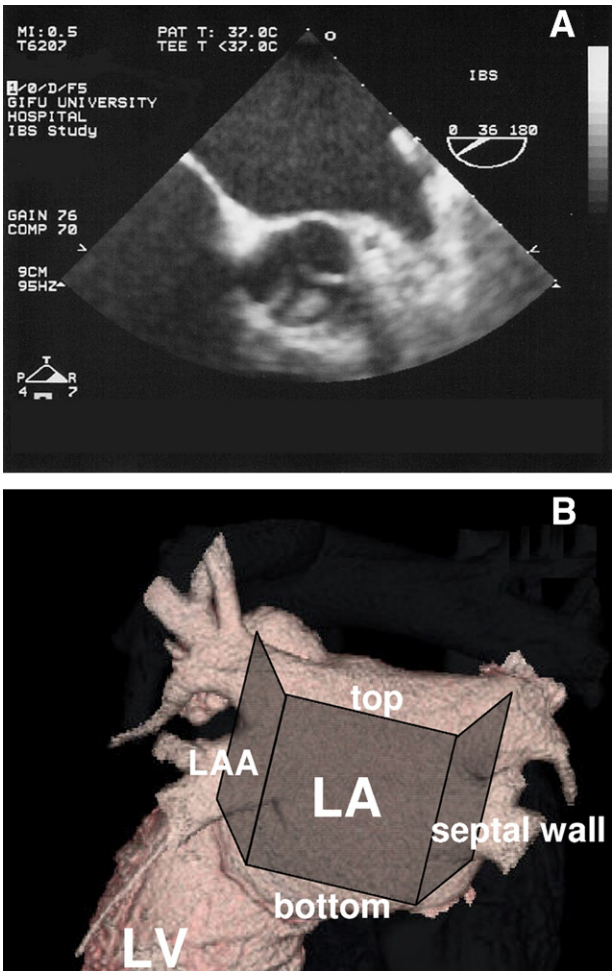

Figure 1. Measurement Site of LA

(A) Cross-sectional image of the left atrium (LA) depicted by transesophageal echocardiography (TEE). Images of the LA were depicted, and integrated backscatter (IBS) values of entire lateral, septal, and anterior walls of the LA were measured at 5-mm intervals. **(B)** Schematic image of the analyzed site **(square)**. Lateral, anterior, and septal walls of the LA were analyzed. LAA = left atrial appendage; LV = left ventricle.

Reproducibility and reliability of data. We previously determined interobserver variability of cIBS values in 30 TEE recordings that were measured by 2 observers at randomly selected cross-sections. The interobserver variability of IBS values was 1.1 ± 3.0% (12). The interobserver correlation coefficient was 0.98 for IBS values. Likewise, we determined intraobserver variability of IBS values in 30 TEE recordings that were measured 2 times by 1 observer

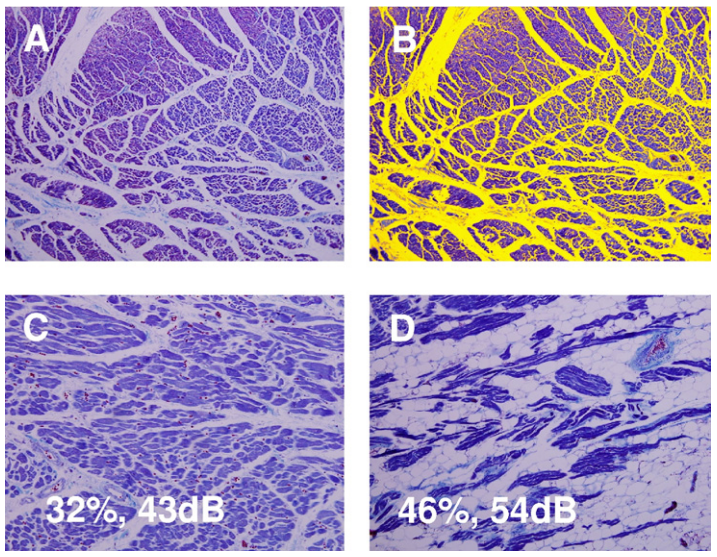

Figure 2. Representative Images in the Pathological Study

(A) Representative histological image of the LA. **(B)** Histological image in which interstitial area was selected **(yellow)** by a multipurpose image processor (LUZEX F, Nireco Co., Tokyo, Japan). **(C)** Representative images of low-grade degeneration of the LA (relative interstitial area: 32%). **(D)** Representative images of high-grade degeneration of the LA (relative interstitial area: 46%).

at randomly selected cross-sections. The intraobserver variability of IBS values was 0.5 ± 3.2%. The intraobserver correlation coefficient was 0.98 for IBS values (12). We determined interobserver variability of average cIBS values in 20 randomly selected color-coded maps that were measured by 2 observers. The intraobserver variability of the average IBS values in color-coded maps was 2.4 ± 2.3%. The interobserver agreements of average IBS values in color-coded maps determined by linear regression was excellent ($r = 0.94$, $p < 0.001$).

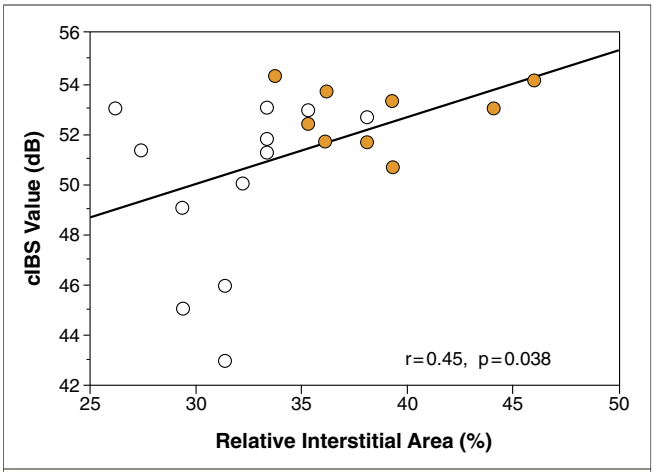

Figure 3. Correlation of Relative Interstitial Area and cIBS Values

As the relative interstitial area of the left atrial (LA) wall became larger, the corrected integrated backscatter (cIBS) values of the LA wall became greater. There was a weak correlation between the relative interstitial area and the average of cIBS values in the LA wall. **Open circles** = patients without atrial fibrillation; **orange circles** = patients with atrial fibrillation.

Statistical analyses. Numerical data are expressed as the mean ± 1 SD. The Kolmogorov-Smirnov test was used to determine whether data were normally distributed. If data were not normally distributed and/or the variances were significantly different (as determined by a Bartlett test), testing for significant differences of each parameter was performed with a Kruskal-Wallis test among 3 groups and a Welch's *t* test between 2 groups. If the data were normally distributed and the variances were not significantly different, the 3 study groups were compared with a 1-way analysis of variance followed by Scheffe's method for post hoc comparisons between individual groups. The relationships among ultrasound parameters and pathological parameters were tested by linear regression analysis. Categorical data were summarized as percentages and compared with a chi-square test. A p value <0.05 was considered to be significant. Statistical analyses were performed with StatView version 5.0 (SAS Institute, Inc., Cary, North Carolina).

RESULTS

Pathological study. Histological images of all specimens were successfully digitized by the multipurpose image processor and were used for the analysis (Fig. 2). There was a weak correlation between the relative interstitial area and the average of cIBS values in LA tissue ($r = 0.45$, $p = 0.038$). As the relative interstitial area with infiltration of fat tissue and disruption of the atrial muscle became larger, the cIBS values of the LA wall became greater (Fig. 3). The average cIBS value in the AF group (52.8 ± 1.2 dB) was significantly greater than that in the non-AF group (49.9 ± 3.5 dB, $p = 0.03$). The relative interstitial area in the AF group (38 ± 4%) was significantly greater than that in the non-AF group (31 ± 3%, $p < 0.001$). The optimum cutoffs for discriminating AF were obtained from the receiver operating characteristic curves analysis (Fig. 4). The optimal cutoffs in the pathological study were 52 dB. The diagnostic accuracies for predicting AF are shown in Table 1.

Patient characteristics in the clinical study. The clinical reasons for TEE examination were: assessment of thrombus in the LA or LAA (n = 29), assessment of valvular disease (n = 8), assessment of congenital heart disease (n = 2), assessment of

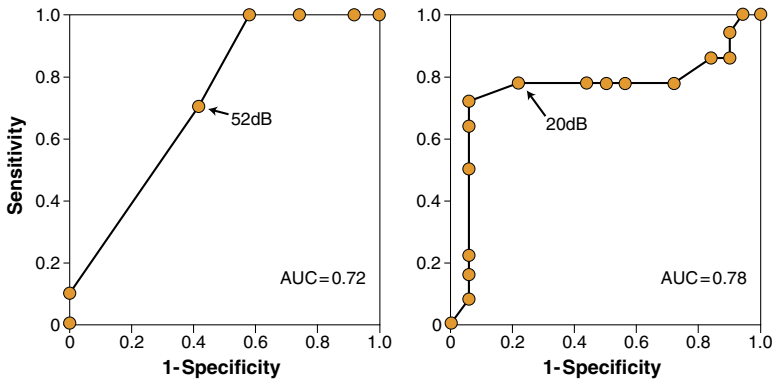

Figure 4. Receiver-Operating Characteristic Curves Analysis for Predicting Atrial Fibrillation

(Left) Pathological study. **(Right)** Clinical study. The optimum cutoffs for discriminating atrial fibrillation were obtained from the receiver operating characteristic curve analysis. The optimal cutoffs were 20 dB in the clinical study and 52 dB in the pathological study. AUC = area under the receiver operating characteristic curve.

suspected infective endocarditis (n = 1), inadequate transthoracic ultrasound examination (n = 1), and assessment of follow-up aortic dissection (n = 1). Baseline clinical characteristics of the patients are shown in Table 2. There were no significant differences among the 3 groups in age, coronary risk factors, and concomitant medication use except for warfarin, angiotensin-converting enzyme inhibitor, and angiotensin II receptor blockers. Medication with warfarin, angiotensin-converting enzyme inhibitor, and angiotensin II receptor blockers was significantly higher in the AF group than in the PAF or non-AF group. All patients completed the study without any complications.

Ultrasound parameters. Ultrasound parameters are shown in Table 3. There was no correlation between LAA peak velocity and IBS values in the LA cavity. Also, there were no significant differences in IBS values of the LA cavity among the 3 groups.

The LAD in the AF group (50.7 ± 7.5 mm, $p < 0.001$) was significantly greater than those in the PAF group (39.4 ± 6.5 mm) and non-AF group (36.7 ± 5.5 mm). The LA volume in the AF group (59.2 ± 18.7 ml) was significantly greater than those in the PAF group (34.5 ± 18.5 ml, $p = 0.003$) and non-AF group (27.4 ± 11.9 ml, $p < 0.001$). There was a weak correlation between the LA volume and the average of cIBS values ($r = 0.34$, $p = 0.026$). There were no significant differences of LV end-diastolic dimension and LV ejection fraction among the 3 groups. The LAA peak velocities in the AF group (26.7 ± 7.5 cm/s, $p = 0.002$) were significantly slower than those in the PAF group (52.3 ± 22.3 cm/s) and non-AF group (55.1 ± 20.8 cm/s). There was no significant difference between LAA peak velocity in the PAF group and LAA peak velocity in the non-AF group, because patients with PAF were in sinus rhythm during TEE. For the IBS analysis, we evaluated a total of 193 ± 87 cIBS values in each patient. Average cIBS values of total pixels in color-coded maps in the AF group (24.4 ± 6.4 dB) and the PAF group (23.9 ± 9.6 dB) were significantly greater than those in the non-AF group (15.6 ± 7.4 dB, $p = 0.007$), whereas there were no significant differences in the LAD and the LA volume between the PAF group and the non-AF group (Fig. 5). The optimum cutoffs for discriminating PAF were obtained from the receiver operating characteristic curve analysis (Fig. 4). The optimal cutoffs in the clinical study were 20 dB. The diagnostic accuracies for predicting AF were shown in Table 1.

Table 1. The Diagnostic Accuracies for Predicting Atrial Fibrillation (Pathological Study) or Paroxysmal Atrial Fibrillation (Clinical Study)

	Sensitivity	Specificity	PPV	NPV
Pathological (n = 21)	67 (47–87)	58 (37–70)	55 (34–76)	70 (50–90)
Clinical (n = 32)	79 (65–93)	78 (64–92)	73 (58–88)	82 (69–95)

Data are presented as % (95% confidence interval).
NPV = negative predictive value; PPV = positive predictive value.

Construction of 3D IBS-TEE color-coded maps. Three-dimensional IBS-TEE color-coded images consisted of a total of 193 ± 87 pixels in each atrium. The area with a high degree of degeneration was indicated by red and yellow colors, and no or a low degree of degeneration was indicated by green and blue colors. The 3D IBS-TEE images allowed

JACC: CARDIOVASCULAR IMAGING, VOL. 2, NO. 9, 2009
SEPTEMBER 2009:1039–47

Table 2. Demographic Data and Baseline Characteristics

	AF (n = 10)	PAF (n = 14)	Non-AF (n = 18)	p Value
Men	7 (70)	12 (86)	16 (89)	0.42
Age (yrs)	64 ± 12	57 ± 10	61 ± 16	0.35
Laboratory parameters (mg/dl)				
ANP	51 ± 29	46 ± 27	39 ± 45	0.71
BNP	200 ± 188	68 ± 85	101 ± 194	0.15
D-dimer	0.97 ± 0.76	0.77 ± 0.20	1.17 ± 1.00	0.48
C-reactive protein	0.38 ± 0.45	0.40 ± 1.05	1.15 ± 2.13	0.34
Clinical history				
Hypertension	8 (80)	9 (64)	9 (50)	0.29
Diabetes mellitus type 2	3 (30)	2 (14)	8 (44)	0.19
Current smoker	1 (10)	5 (36)	5 (28)	0.36
Dyslipidemia	3 (30)	3 (21)	7 (39)	0.57
Medication				
Warfarin	8 (80)*	6 (43)	5 (50)	0.03
Aspirin	3 (30)	4 (29)	7 (39)	0.80
Ticlopidine	0 (0)	1 (7)	1 (6)	0.70
Diuretic	2 (20)	2 (14)	1 (6)	0.50
Calcium channel blockers	4 (40)	4 (29)	5 (28)	0.78
Beta-blockers	4 (40)	4 (29)	3 (17)	0.39
ACE inhibitors or ARBs	9 (90)*	6 (43)	7 (39)	0.02

*Significant difference. Data are presented as n (%) or mean ± 1 SD.
ACE = angiotensin-converting enzyme; AF = atrial fibrillation; ANP = atrial natriuretic peptide; ARB = angiotensin II receptor blocker; BNP = brain natriuretic peptide; PAF = paroxysmal atrial fibrillation.

visualization of LA degeneration as signified by a red color in the color-coded maps (Fig. 6). By looking at these images, we were easily able to identify the location of areas of degeneration in the LA wall.

DISCUSSION

The findings in the present study demonstrated that a larger interstitial area of LA tissue was associated with greater IBS values in the pathological study and IBS values in patients with chronic AF and PAF were greater than those in patients without AF. However, the LAD was similar in patients with PAF and in those without AF. These findings indicated that the LA myocardium in patients with PAF had already degenerated before the enlargement of the LA. Therefore, we could predict the patients who were likely to progress from non-AF to PAF or chronic AF. To the best of our knowledge, this is the first pilot study to elucidate clinically the tissue characteristics of the LA by use of IBS-TEE.

Table 3. Ultrasound Parameters of the Patients

	AF (n = 10)	PAF (n = 14)	Non-AF (n = 18)	p Value
LAD (mm)	50.0 ± 7.5	39.4 ± 6.5*	36.7 ± 5.5*	<0.001
LA volume (ml)	59.2 ± 18.7	34.5 ± 18.5*	27.4 ± 11.9*	<0.001
LVEDD (mm)	49.2 ± 5.3	47.2 ± 4.7	50.7 ± 7.7	0.31
LVEF (%)	63.5 ± 10.8	67.9 ± 7.1	61.5 ± 9.4	0.15
LAA peak velocity (cm/s)	26.7 ± 7.5	52.3 ± 22.3*	55.1 ± 20.8*	0.002
Corrected IBS value (dB)	24.4 ± 6.4†	23.9 ± 9.6†	15.6 ± 7.4	0.007

Values are mean ± 1 SD. *$p < 0.01$ versus the atrial fibrillation (AF) group. †$p < 0.05$ versus the non-AF group.
IBS = integrated backscatter; LA = left atrium; LAA = left atrial appendage; LAD = left atrial dimension; LVEDD = left ventricular end-diastolic dimension; LVEF = left ventricular ejection fraction; PAF = paroxysmal atrial fibrillation.

Detecting the degeneration of LA tissue. It is noteworthy that the LA in the patients with PAF had already degenerated before the enlargement of the LA. LA enlargement is part of cardiac remodeling observed in various cardiovascular diseases and associated with increased risk of cardiac death (13,14). Atrial fibrillation leads to reduction of atrial contraction and an increase of mitral regurgitation. Mitral regurgitation leads to atrial stretch and LA dilation (15). It is well known that an increased LA diameter leads to a higher incidence of AF (16). In the present study, AF patients had greater LA size and IBS values; however, there was no significant difference of LA diameter and LA volume between patients with PAF and non-AF patients, despite a significant difference between chronic AF and non-AF patients. The present findings demonstrated a significant difference of atrial degeneration between patients with PAF and non-AF patients. The present results might explain 1 of the mechanisms for the continuation of AF—that is, AF leads to atrial histological remodeling and then atrial stretch. The stretched atrial tissue is associated with an increased arrhythmogenic activity and LA dilation, and this contributes to the continuation of AF (17–19).

Previous studies have reported that treatment with angiotensin-converting enzyme inhibitors or angiotensin II receptor blockers can delay the progression of PAF to chronic AF (20–22). The findings of the present study suggest that it might be possible to prevent the progression of non-AF to chronic AF by detecting the patients with high degree of LA degeneration and initiating treatment with angiotensin-converting enzyme inhibitors or angiotensin II receptor blockers.

Pathological study. The IBS values obtained from ultrasound radiofrequency signal analysis of the arteries obtained at autopsy reflect the acoustic characteristics of the wall and can differentiate among the tissue characteristics of arterial plaques (5,6). Ultrasound backscatter power was proportional to the difference of acoustic characteristic impedance that was determined by the density of tissue multiplied by the speed of sound. Because of

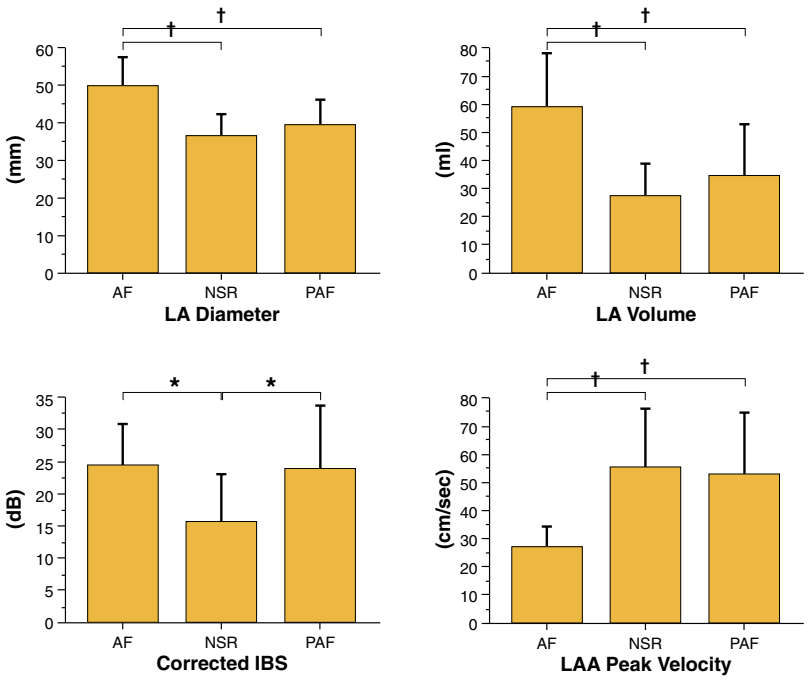

Figure 5. Ultrasound Parameters of Chronic AF, PAF, and NSR Groups

Average corrected integrated backscatter (IBS) values of total pixels in color-coded maps in the atrial fibrillation (AF) group and the paroxysmal atrial fibrillation (PAF) group were significantly greater than those in the normal sinus rhythm (NSR) group, whereas there were no significant differences in the left atrial (LA) diameter, the LA volume, and left atrial appendage (LAA) peak velocity between the PAF group and the NSR group. $*p < 0.05$; $†p < 0.01$.

the complex geometry of the LA, the acoustic characteristic impedance is highly variable. Therefore, we hypothesized that it was possible to evaluate the degeneration of LA tissue by applying IBS analysis to TEE. First, we performed a pathological study comparing atrial tissue and IBS values ex vivo, because it was reported that there was no significant influence of formalin fixation on acoustic characteristic impedance, whereas formalin fixation decreased distensibility significantly in noncalcified arterial tissue (23,24). In the present study, as the relative interstitial area became larger, cIBS values of the LA wall became greater. Cardiac remodeling, especially in the LA, is more pronounced in patients

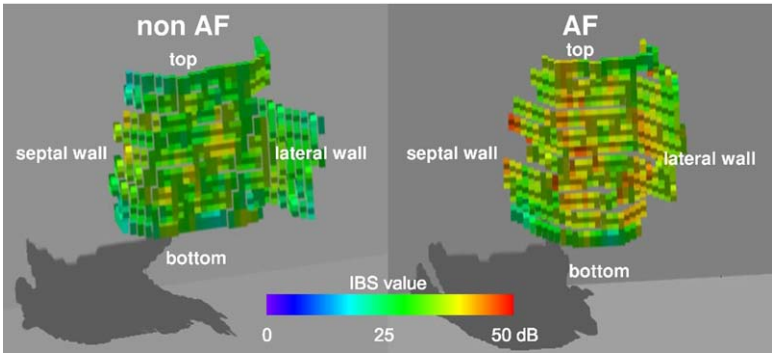

Figure 6. Three-Dimensional IBS Color-Coded Maps of the LA

The area of a high degree of degeneration was indicated by **red** and **yellow** colors, and no or a low degree of degeneration was indicated by **green** and **blue** colors. By looking at these images, we were easily able to identify the location of areas of degeneration in the LA wall. Abbreviations as in Figure 5.

with AF. This explanation is supported by an autopsy study that demonstrated increased amount of fibrosis in the atria of patients with AF compared with patients in sinus rhythm (15). Another report demonstrated that some of the histological features of the LA in patients with AF were an increase in interstitial tissue with infiltration of fatty tissue, interstitial fibrosis, and disruption of the atrial muscle (3). The atrium is more susceptible to fibrosis than the ventricle, although the precise mechanisms involved in the development of atrial fibrosis are currently unknown (25).

Technical consideration. Because it is considered that attenuation and the reverberation phenomena had an effect in evaluation of IBS values of the atrial wall in the present ex vivo and in vivo studies, the reverberation phenomena should be excluded for precise comparison of the IBS values. Therefore, we corrected the IBS values of the atrial wall by subtracting the IBS values of the atrial cavity with saline in the ex vivo study and with flowing blood in the in vivo study, because the same method has been performed in myocardial tissue characterization with IBS (26). Ultrasound study reported that decreasing LAA blood velocity was associated with increasing grades of spontaneous echo contrast in LA (27,28). In the present study, however, there was no correlation between LAA velocity and IBS values near the LA wall. Therefore, correcting the method in the present study was not likely to affect the results of determining each cIBS value.

Study limitations. There are several limitations of the present study. First, because the number of patients in our analysis was small and the clinical end point of chronic AF could not be evaluated prospectively, the sensitivity and specificity to predict the incidence of chronic AF could not be evaluated. Prospective follow-up studies, which include an analysis of the incidence of chronic AF, will be required in the future. Second, we did not analyze IBS values of LA tissue separating the patients with lone AF and the patients with AF due to mitral valve regurgitation, whereas we excluded patients with AF due to mitral valve stenosis from the study. Volume overload in LA due to mitral valve regurgitation is more likely to stretch the LA than the presence of lone AF. The pattern of atrial remodeling in patients with mitral valve regurgitation might be different from that in patients with lone AF. Third, this study was an incidental study of valvular and other cardiac disease. Therefore, the findings of the present study might not be applicable to the general population. Finally, color-coded maps were constructed manually and took several minutes to construct. Future development of real-time construction of color-coded maps is required for clinical practice by developing original computer software.

CONCLUSIONS

The TEE applied IBS method is generally safe and useful to assess LA degeneration. With IBS-TEE, we can identify an increase in degeneration in the LA wall in patients with PAF and chronic AF and might be able to predict the occurrence of chronic AF before LA dilation.

Reprint requests and correspondence: Dr. Masanori Kawasaki, Regeneration and Advanced Medical Science, Gifu University Graduate School of Medicine, 1-1 Yanagido, Gifu 501-1194, Japan. *E-mail: masanori@ya2.so-net.ne.jp.*

REFERENCES

1. Feinberg WM, Blackshear JL, Laupacias A, et al. Prevalence, age distribution and gender of patients with atrial fibrillation: analysis and implications. Arch Intern Med 1995;155:469–73.
2. Kostin S, Klein G, Szalay Z, et al. Structural correlate of atrial fibrillation in human patients. Cardiovasc Res 2002;54:361–79.
3. Bharati S, Lev M. Histology of the normal and diseased atrium. In: Falk HE, Podrid PJ, editors. Atrial Fibrillation and Management. New York, NY: Raven Press, Ltd., 1992:15–39.
4. Frustaci A, Chimenti C, Bellocci F, et al. Histological substrate of atrial biopsies in patients with lone atrial fibrillation. Circulation 1997;96:1180–4.
5. Kawasaki M, Takatsu H, Noda T, et al. Noninvasive quantitative tissue characterization and two-dimensional color-coded map of human atherosclerotic lesions using ultrasound integrated backscatter: comparison between histology and integrated backscatter images. J Am Coll Cardiol 2001;38:486–92.
6. Kawasaki M, Ito Y, Yokoyama H, et al. Assessment of arterial medial characteristics in human carotid arteries using integrated backscatter ultrasound and its histological implications. Atherosclerosis 2005;180:145–54.
7. Picano E, Pelosi G, Marzilli M, et al. In vivo quantitative ultrasonic evaluation of myocardial fibrosis in humans. Circulation 1990;81:58–64.
8. Naito J, Masuyama T, Mano T, et al. Ultrasonic myocardial tissue characterization in patients with dilated cardiomyopathy: value in noninvasive assessment of myocardial fibrosis. Am Heart J 1996;131:115–21.
9. Lang RM, Bierig M, Devereux RB, et al. Recommendations for Chamber Quantification: a report from the American Society of Echocardiography's Guidelines and Standards Committee and the Chamber Quantification Writing Group, developed in conjunction with the European Association of Echocardiography, a branch of the European Society of Cardiology. J Am Soc Echocardiogr 2005;18:1440–63.
10. Picano E, Landdini L, Distante A, Salvadori M, L'Abbate A. Angle dependence of ultrasonic backscatter in arterial tissues: a study in vitro. Circulation 1985;72:572–6.

11. Okubo M, Kawasaki M, Ishihara Y, et al. Development of integrated backscatter intravascular ultrasound for tissue characterization of coronary plaques. Ultrasound Med Biol 2008; 34:655–63.
12. Ono K, Kawasaki M, Tanaka R, et al. Integrated backscatter and intima-media thickness of the thoracic aorta evaluated by transesophageal echocardiography in hypercholesterolemic patients: effect of pitavastatin therapy. Ultrasound Med Biol 2009;35:193–200.
13. Grigioni F, Avierinos JF, Ling LH, et al. Atrial fibrillation complicating the course of degenerative mitral regurgitation: determinants and long-term outcome. J Am Coll Cardiol 2002;40:84–92.
14. Benjamin EJ, D'Agostino RB, Belanger AJ, et al. Left atrial size and the risk of stroke and death. The Framingham Heart Study. Circulation 1995;92: 835–41.
15. Kostin S, Klein G, Szalay Z, Hein S, Bauer EP, Schaper J. Structural correlate of atrial fibrillation in human patients. Cardiovasc Res 2002;54:361–79.
16. Fraser HR, Turner RW. Auricular fibrillation; with special reference to rheumatic heart disease. Br Med J 1955;4953:1414–8.
17. Spach MS, Josephson ME. Initiating reentry: the role of nonuniform anisotropy in small circuits. J Cardiovasc Electrophysiol 1994;5:182–209.
18. Franz MR. Mechano-electrical feedback. Cardiovasc Res 2000;45:263–6.
19. Ruwhof C, van der Laarse A. Mechanical stress-induced cardiac hypertrophy: mechanisms and signal transduction pathways. Cardiovasc Res 2000;47:23–37.
20. Vermes E, Tardif JC, Bourassa MG, et al. Enalapril decreases the incidence of atrial fibrillation in patients with left ventricular dysfunction: insight from the Studies of Left Ventricular Dysfunction (SOLVD) trials. Circulation 2003;107:2926–31.
21. Wachtell K, Lehto M, Gerdts E, et al. Angiotensin II receptor blockade reduces new-onset atrial fibrillation and subsequent stroke complication to atenolol. J Am Coll Cardiol 2005;45: 712–9.
22. Maggioni AP, Latini R, Carson PE, et al. Valsartan reduces the incidence of atrial fibrillation in patients with heart failure: results from the Valsartan Heart Failure Trial (Val-HeFT). Am Heart J 2005;149:548–57.
23. Park JC, Siegel RJ, Demer LL. Effect of calcification and formalin fixation on in vitro distensibility of human femoral arteries. Am Heart J 1993;125:344–9.
24. Picano E, Landini L, Distante A, et al. Different degrees of atherosclerosis detected by backscattered ultrasound: an in vitro study on fixed human aortic walls. J Clin Ultrasound 1983;11:375–9.
25. Thomas H, Everett IV, Jeffrey E, et al. Atrial fibrosis and the mechanisms of atrial fibrillation. Heart Rhythm 2007;4:S24–7.
26. Naito J, Masuyama T, Mano T, et al. Ultrasound myocardial tissue characterization in the patients with dilated cardiomyopathy: value in noninvasive assessment of myocardial fibrosis. Am Heart J 1996;131:115–21.
27. Fatkin D, Kelly RP, Feneley MP. Relations between left atrial appendage blood flow velocity, spontaneous echocardiographic contrast and thromboembolic risk in vivo. J Am Coll Cardiol 1994;23:961–9.
28. Tsai LM, Chao TH, Chen JH. Association of follow-up change of left atrial appendage blood flow velocity with spontaneous echo contrast in nonrheumatic atrial fibrillation. Chest 2000;117:309–13.

Key Words: atrial fibrillation ■ integrated backscatter ■ tissue characterization ■ transesophageal echocardiography.